

Solvothermal Syntheses, Crystal Structures, and Properties of New $[\text{Mn}(\text{dien})_2]^{2+}$ Complexes

Jan Ellermeier and Wolfgang Bensch*

Institut für Anorganische Chemie, Christian-Albrechts-Universität Kiel, D-24098-Kiel, Germany

Summary. The two new compounds $\text{Mn}(\text{dien})_2[\text{MoS}_4]$ (**1**) and $\text{Mn}(\text{dien})_2[\text{Mo}_2\text{O}_2\text{S}_6]$ (**2**) (*dien* = diethylenetriamine) were prepared under solvothermal conditions. Both compounds were obtained as phase-pure products. The structures consist of new $[\text{Mn}(\text{dien})_2]^{2+}$ cations and isolated tetrahedral $[\text{MoS}_4]^{2-}$ (**1**) or $[\text{Mo}_2\text{O}_2\text{S}_6]^{2-}$ (**2**) anions. Between the anions and the cations, hydrogen bonding is observed. Compound **1** crystallizes in the tetragonal space group $\bar{I}4$ ($a = 10.219(2)$, $c = 9.259(2)$ Å, $Z = 2$), whereas **2** crystallizes in the monoclinic space group $P2_1/c$ ($a = 8.703(2)$, $b = 18.390(4)$, $c = 14.603(3)$ Å, $\beta = 103.18(3)^\circ$, $Z = 4$). The thermal behaviour of the thiomolybdates was investigated using difference thermoanalysis (DTA) and thermogravimetry (TG). Both compounds decompose under argon with a single endothermic signal in the DTA curve (peak maximum: 252 (**1**) and 242°C (**2**)).

Keywords. Thiomolybdates; Solvothermal synthesis; Crystal structure; Physical properties.

Introduction

The application of hydro- and solvothermal methods in solid state chemistry has produced a large number of compounds with new structural features ranging from discrete molecular anions to three-dimensional frameworks. Often the compounds show highly interesting physical properties [1–3]. One important advantage of the solvothermal method is that the crystals are of good quality, and in most cases phase-pure products are obtained.

The large interest in the field of thiomolybdate chemistry is above all a result of the observation that Mo–S coordination in molybdenum-containing enzymes plays an important role [4]. Furthermore, molybdenum sulfides are the active components in hydrodesulfurization (HDS) and other hydrotreating catalysts which are used for the purification of petroleum products [5]. Several thio- and oxothiomolybdate anions have been described in the literature [6], and the anionic Mo_xS_y species range from the tetrahedral $[\text{MoS}_4]^{2-}$ anion to very complex moieties like in $\text{Rb}_{10}\text{Mo}_{36}\text{S}_{38}$ [7]. The multitude of thiomolybdates is completed by a large number of bi- and trinuclear molybdenum clusters like the $[\text{Mo}_3\text{S}_{13}]^{2-}$ anion

* Corresponding author. E-mail: wbensch@ac.uni-kiel.de

[8]. The oxothiomolybdates form a series with general composition $[\text{MoO}_{4-n}\text{S}_n]^{2-}$ ($n = 0-4$), but complex multinuclear anions like $[\text{Mo}_4\text{O}_4\text{S}_{14}]^{2-}$ [9], $[\text{Mo}_4\text{O}_4\text{S}_{18}]^{2-}$ [10, 11], and $[\text{Mo}_6\text{O}_6\text{S}_{14}]^{4-}$ [12] have also been reported.

The interest in octahedral $[\text{M}(\text{dien})_2]^{n+}$ complexes with the tridentate ligand diethylenetriamine (*dien*) originates from their possibility of generating three geometrical isomeric forms: meridional (*mer*), symmetrical facial (*s-fac*), and unsymmetrical facial (*u-fac*) [13]. Bis-*dien* complexes have been described for various transition metal ions like cobalt(III) [14–16], chromium(III) [17–18], rhodium(III) [19], iridium(III) [19], iron(II) [20], nickel(II) [21–25], copper(II) [26], and zinc(II) [27]. However, to the best of our knowledge, a single crystal structural characterization of manganese(II) bis-*dien* complexes has not yet been published. Herein, we report on the *mer* and *u-fac* forms of $[\text{Mn}(\text{dien})_2]^{2+}$ together with the solvothermal syntheses, crystal structures, and thermal and vibrational properties of $\text{Mn}(\text{dien})_2[\text{MoS}_4]$ (**1**) and $\text{Mn}(\text{dien})_2[\text{Mo}_2\text{O}_2\text{S}_6]$ (**2**).

Results and Discussion

Crystal structures

$\text{Mn}(\text{dien})_2[\text{MoS}_4]$ (**1**, *dien* = diethylenetriamine) crystallizes in the tetragonal space group $I\bar{4}$ with two formula units in the unit cell; $\text{Mn}(\text{dien})_2[\text{Mo}_2\text{O}_2\text{S}_6]$ (**2**) crystallizes in the monoclinic space group $P2_1/c$ with four formula units in the unit cell. Compound **2** is isostructural to the recently published $\text{Ni}(\text{dien})_2[\text{Mo}_2\text{O}_2\text{S}_6]$ [25]. The Mn atoms in **1** and **2** are in a distorted octahedral environment of six N atoms from the *dien* ligands, forming $[\text{Mn}(\text{dien})_2]^{2+}$ cations. Therefore, the structures consist of $[\text{Mn}(\text{dien})_2]^{2+}$ cations and tetrahedral $[\text{MoS}_4]^{2-}$ anions in **1** and discrete dimeric $[\text{Mo}_2\text{O}_2\text{S}_6]^{2-}$ anions in **2**. Selected interatomic distances are listed in Table 1 for $\text{Mn}(\text{dien})_2[\text{MoS}_4]$ and in Table 2 for $\text{Mn}(\text{dien})_2[\text{Mo}_2\text{O}_2\text{S}_6]$.

The *dien* molecules act as tridentate ligands, and three geometrical isomers are possible: *mer*, *s-fac*, and *u-fac*. The $[\text{Mn}(\text{dien})_2]^{2+}$ cation in **1** (see Fig. 1) shows the meridional geometry. The *trans*-angle N2–Mn–N2 involving the terminal nitrogen atoms is $152.6(2)^\circ$; with the secondary nitrogen atoms (N1–Mn–N1), the angle is 180° being restricted by symmetry. The four symmetry-related primary N2 atoms and the Mn(II) ion deviate from a calculated best-plane, two N2 atoms being 0.544 Å above and two N2 atoms being 0.544 Å below the idealized plane. In contrast to the meridional form in **1**, the $[\text{Mn}(\text{dien})_2]^{2+}$ cation in **2** (see Fig. 2) prevails in the unsymmetrical facial (*u-fac*) form. The terminal amino groups within the *dien* ligands are in *cis*-positions (N1–Mn–N3 = $99.36(9)^\circ$, N4–Mn–N6 = $106.40(9)^\circ$),

Table 1. Selected distances (Å) and angles ($^\circ$) for $\text{Mn}(\text{dien})_2[\text{MoS}_4]$ (**1**); estimated standard deviations are given in parentheses

Mo–S	2.1765(8) (x 4)		
S–Mo–S	109.50(3) (x 4)	S–Mo–S	109.41(7) (x 2)
Mn–N(1)	2.233(5) (x 2)	Mn–N(2)	2.298(3) (x 4)
N(1)–Mn–N(2)	103.68(7) (x 4)	N(1)–Mn–N(2)	76.32(7) (x 4)
N(2)–Mn–N(2)	93.21(3) (x 4)	N(2)–Mn–N(2)	152.6(2) (x 2)

Table 2. Selected distances (Å) and angles (°) for Mn(*dien*)₂[Mo₂O₂S₆] (**2**); estimated standard deviations are given in parentheses

Mo(1)–O(1)	1.694(2)	Mo(2)–O(2)	1.690(2)
Mo(1)–S(1)	2.319(1)	Mo(1)–S(2)	2.323(1)
Mo(1)–S(3)	2.373(1)	Mo(1)–S(4)	2.415(1)
Mo(2)–S(1)	2.340(2)	Mo(2)–S(2)	2.317(1)
Mo(2)–S(5)	2.392(1)	Mo(2)–S(6)	2.393(1)
S(3)–S(4)	2.071(2)	S(5)–S(6)	2.076(2)
Mo(1)–Mo(2)	2.818(1)		
Mn–N(1)	2.237(2)	Mn–N(2)	2.311(2)
Mn–N(3)	2.326(2)	Mn–N(4)	2.302(2)
Mn–N(5)	2.319(2)	Mn–N(6)	2.258(2)
O(1)–Mo(1)–S(1)	110.00(8)	O(1)–Mo(1)–S(2)	107.00(7)
O(1)–Mo(1)–S(3)	114.83(7)	O(1)–Mo(1)–S(4)	105.98(7)
O(2)–Mo(2)–S(1)	109.14(8)	O(2)–Mo(2)–S(2)	108.34(9)
O(2)–Mo(2)–S(5)	109.30(8)	O(2)–Mo(2)–S(6)	112.10(9)
S(1)–Mo(1)–S(2)	103.14(3)	S(1)–Mo(1)–S(3)	127.52(3)
S(1)–Mo(1)–S(4)	91.57(3)	S(2)–Mo(1)–S(3)	88.76(4)
S(2)–Mo(1)–S(4)	136.30(3)	S(3)–Mo(1)–S(4)	51.26(4)
S(2)–Mo(2)–S(1)	102.69(3)	S(1)–Mo(2)–S(5)	133.49(3)
S(1)–Mo(2)–S(6)	90.01(3)	S(2)–Mo(2)–S(5)	89.05(3)
S(2)–Mo(2)–S(6)	130.49(3)	S(5)–Mo(2)–S(6)	51.42(3)
Mo(1)–S(1)–Mo(2)	74.45(2)	Mo(2)–S(2)–Mo(1)	74.81(2)
N(1)–Mn–N(2)	77.19(8)	N(1)–Mn–N(3)	99.36(9)
N(1)–Mn–N(4)	92.76(9)	N(1)–Mn–N(5)	165.04(8)
N(1)–Mn–N(6)	97.44(9)	N(2)–Mn–N(3)	75.03(8)
N(4)–Mn–N(2)	91.43(8)	N(2)–Mn–N(5)	112.52(7)
N(6)–Mn–N(2)	161.70(9)	N(4)–Mn–N(3)	159.19(9)
N(5)–Mn–N(3)	94.30(8)	N(6)–Mn–N(3)	88.83(9)
N(4)–Mn–N(5)	76.10(8)	N(6)–Mn–N(4)	106.40(9)
N(6)–Mn–N(5)	76.66(8)		

as are the secondary amino groups with an N2–Mn–N5 angle of 112.52(7)°. The distortion of the octahedral environment is also obvious from the *trans*-N–Mn–N angles which range from 159.19(9) to 165.04(8)°.

The Mn–N distances in **1** are 2.233(5) and 2.298(3) Å. They range from 2.237(2) to 2.326(2) Å in the [Mn(*dien*)₂]²⁺ cation of **2** and are elongated compared to the isostructural *u-fac* [Ni(*dien*)₂]²⁺ cation [25] in accordance with the larger ionic radius of Mn²⁺. The Mn–N distances found in the new [Mn(*dien*)₂]²⁺ cations are comparable to those reported for the [Mn(*en*)₃]²⁺ cation (*en* = 1,2-ethanediamine) [28, 29].

The counterion in **1** is the tetrahedral [MoS₄]²⁻ anion. The S–Mo–S angles deviate only slightly from the value for an ideal tetrahedron (109.41(7) to 109.50(3)°), and the corresponding bond length is 2.177(1) Å. These values are normal and have also been found in other compounds [30–33]. The discrete [Mo₂O₂S₆]²⁻ anion in **2** is built up of a Mo₂S₂O₂ core which is completed by

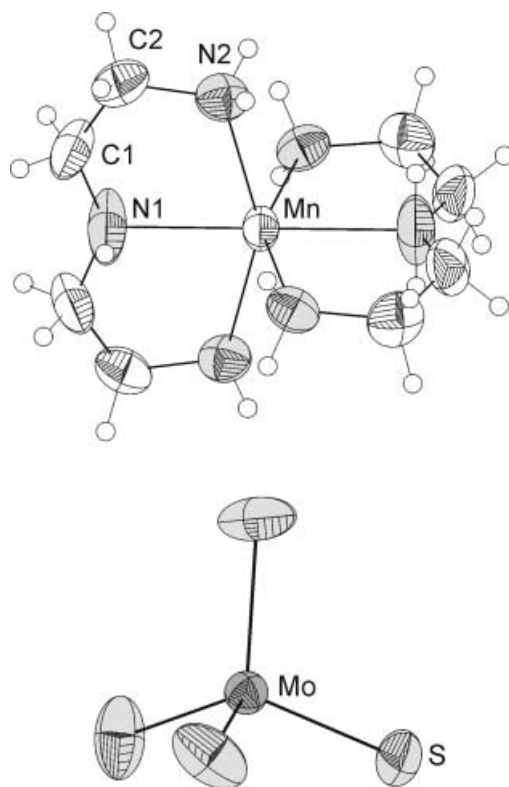


Fig. 1. View of $[\text{Mn}(\text{dien})_2]^{2+}$ and $[\text{MoS}_4]^{2-}$ in **1** with labelling and displacement ellipsoids drawn at the 50% probability level (disordered C atoms are omitted for clarity; the H atom attached to N1 is distributed over two positions)

two $\eta^2\text{-S}_2^{2-}$ groups (see Fig. 2) with S–S distances of 2.071(2) Å for S3–S4 and 2.076(2) Å for S5–S6. The mean Mo=O bond length is 1.692(2) Å and is comparable to the Mo=O distances found in other $[\text{Mo}_2\text{O}_2\text{S}_6]^{2-}$ anions [25, 33–36]. Two kinds of Mo–S bonds are observed in the anion; the average Mo–S distance to the bridging $\mu_2\text{-S}$ atoms is 2.325(2) Å, whereas the bond lengths to the terminal S atoms range from 2.373(1) to 2.415(1) Å. The Mo–Mo separation of 2.818(1) Å is in agreement with values reported in the literature.

The arrangement of cations and anions in **1** is depicted in Fig. 3a. The tetrahedral $[\text{MoS}_4]^{2-}$ anions are located on the cell corners and in the centre of the tetragonal cell. The $[\text{Mn}(\text{dien})_2]^{2+}$ cations are located between the anions with one secondary N atom being near the middle of the *a*- and *b*-axis, and the central Mn(II) ions are moved by $\pm 1/4$ in the direction of the *c*-axis. Considering only the Mo and Mn atoms, the structure may be viewed as two interpenetrating independent body centred tetragonal cells (Fig. 3b). Short intermolecular contacts between the hydrogen atoms of the primary amino atoms and the sulfur atoms are observed indicating hydrogen bonding (Table 3).

Compound **2** is isostructural to the recently reported $\text{Ni}(\text{dien})_2[\text{Mo}_2\text{O}_2\text{S}_6]$ [25], and the arrangement of the anions and cations in the crystal structure is shown in Fig. 4. The $[\text{Mn}(\text{dien})_2]^{2+}$ cations and the $[\text{Mo}_2\text{O}_2\text{S}_6]^{2-}$ anions are connected *via* hydrogen bonding (Table 3). According to the interatomic distances and angles,

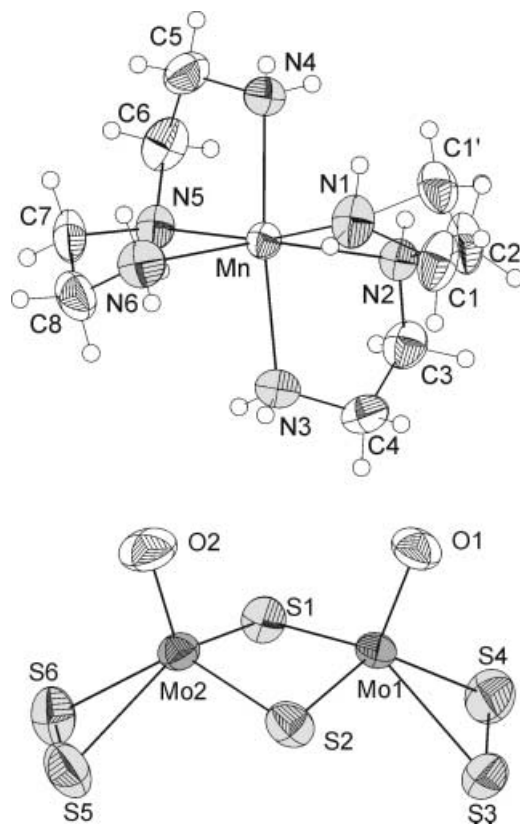


Fig. 2. View of $[\text{Mn}(\text{dien})_2]^{2+}$ and $[\text{Mo}_2\text{O}_2\text{S}_6]^{2-}$ in **2** with labelling and displacement ellipsoids drawn at the 50% probability level (C1' is a split position of C1)

both oxygen and sulfur atoms are involved in intermolecular hydrogen bonding. The $\text{O} \cdots \text{H}$ separations (2.36, 2.58, and 2.59 Å) are, as expected, noticeable shorter than the $\text{S} \cdots \text{H}$ distances which range from 2.63 to 2.93 Å.

Thermal investigations

Experiments conducted with simultaneous difference thermoanalysis (DTA) and thermogravimetry (TG) yielded information about the thermal stability of the compounds. The DTA curves of both compounds exhibit only one strong endothermic signal. Compound **1** starts to decompose at 230°C with a maximum of the large endothermic signal at 252°C (Fig. 5). The corresponding weight loss of 39.7% is significantly lower than expected for the complete removal of the *dien* ligands ($\Delta m_{\text{theor}} = 49.1\%$ for the formation of MnS and MoS₂). In the dark-grey residue, significant amounts of C, H, and N were detected (C: 7.74%, H: 0.28%, N: 3.10%; CHN_{sum} : 11.12%). The strong contamination with carbon is probably due to the formation of MoS_{2-y}C_z compounds [37]. In the X-ray powder pattern only MnS could be identified, suggesting that the other decomposition products are amorphous.

Compound **2** is stable up to 225°C under an argon atmosphere before decomposition starts. The decomposition is accompanied by a large endothermic signal in the DTA curve with a peak maximum at 242°C (Fig. 6). In contrast to the sharp

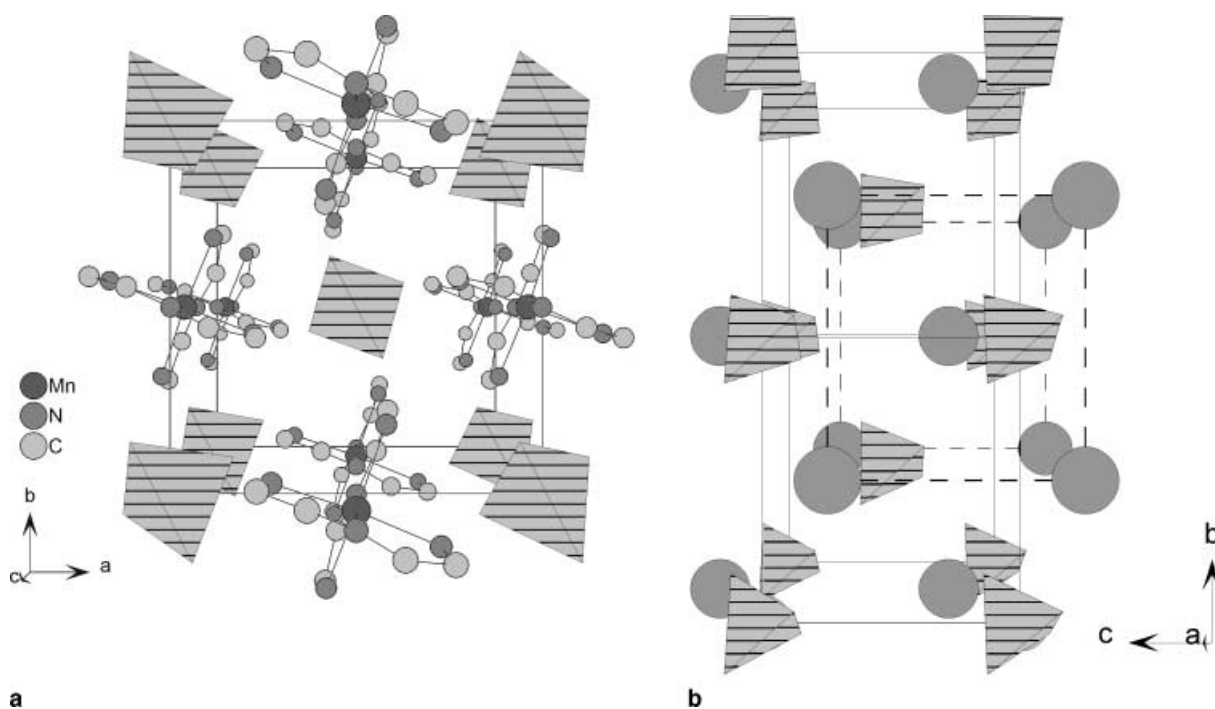


Fig. 3. a) Crystal structure of $\text{Mn}(\text{dien})_2[\text{MoS}_4]$ viewed along the c -axis (H atoms and disordered atoms are omitted for clarity); b) schematical view of the crystal structure of $\text{Mn}(\text{dien})_2[\text{MoS}_4]$ along the a -axis; note: $[\text{MoS}_4]^{2-}$ anions are displayed as tetrahedra, $[\text{Mn}(\text{dien})_2]^{2+}$ cations as grey spheres; the dotted line highlights the body-centred arrangement of the cations

Table 3. Shortest interatomic $\text{S} \cdots \text{H}$ and $\text{O} \cdots \text{H}$ separations (\AA) and corresponding angles ($^\circ$)

$D\text{-H}$	A	$d(\text{H} \cdots A)$	$\angle \text{DHA}$	$d(D \cdots A)$	
a) $\text{Mn}(\text{dien})_2[\text{MoS}_4]$ (1)					
N2-H2a	S	2.70	172.3	3.60	$(y-1, -x+1, -z+1)$
N2-H2b	S	2.90	134.6	3.59	$(-x+1/2, -y+3/2, z+1/2)$
b) $\text{Mn}(\text{dien})_2[\text{Mo}_2\text{O}_2\text{S}_6]$ (2)					
N1-H1a	S4	2.88	113.9	3.35	$(x+1, -y+1/2, z+1/2)$
N1-H1b	S6	2.65	168.5	3.53	$(-x+1, -y+1, -z+1)$
N2-H2	S1	2.92	148.1	3.72	$(x, -y+1/2, z+1/2)$
N3-H3a	O2	2.59	136.9	3.30	$(-x+1, -y+1, -z+1)$
N3-H3b	O2	2.58	160.7	3.45	
N4-H4a	S3	2.84	176.9	3.74	$(x+1, -y+1/2, z+1/2)$
N4-H4b	O1	2.36	169.9	3.25	$(x, -y+1/2, z+1/2)$
N5-H5	S2	2.80	160.0	3.67	
N6-H6a	S5	2.63	176.2	3.53	$(-x+1, -y+1, -z+1)$
N6-H6b	S1	2.93	158.6	3.78	$(x+1, -y+1/2, z+1/2)$

weight loss of **1**, the thermogravimetry curve of **2** shows a strong weight loss immediately after the beginning of the decomposition, followed by a continuous mass reduction up to about 500°C (the highest temperature applied in the experiment).

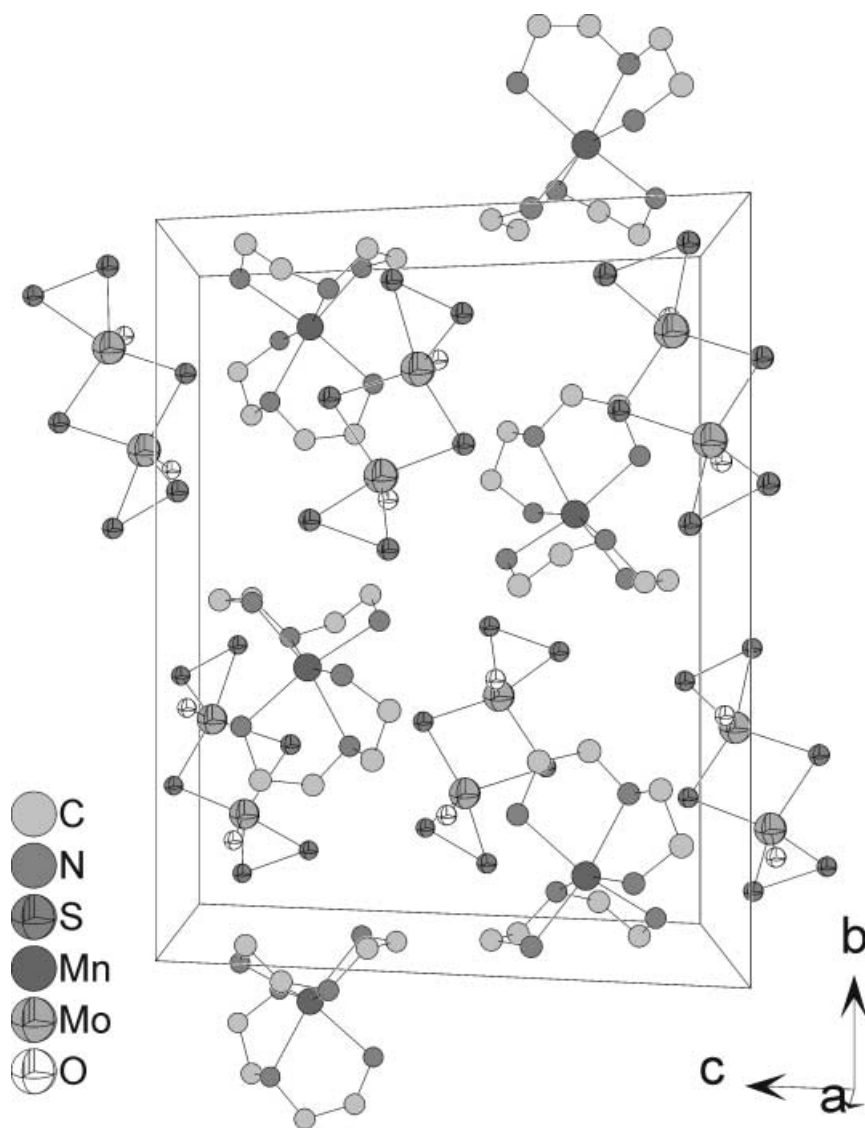


Fig. 4. Crystal structure of Mn(dien)₂[Mo₂O₂S₆] viewed along the *a*-axis (H atoms and disordered atoms are omitted for clarity)

The total mass change amounts to 24.2%. Assuming that all *dien* ligands are emitted during the thermal reaction, a significantly larger weight loss of 35.2% is expected assuming the formation of MnS and 2 MoOS₂ ($\Delta m_{\text{theor}} = 39.9\%$ for the formation of MnS and 2 MoS₂). It is noted that the thermal decomposition of oxothiomolybdates like (NH₄)₂MoO₂S₂ yields MoOS₂ as an intermediate product, but the exact composition of the oxysulfide is not clear [38]. In the X-ray powder diffraction pattern of the residue of **2**, only the reflections of MnS and an unidentified broad signal are observed. The powder diffraction pattern of the decomposition products of **1** and **2** are very similar, even though the anions in the compounds are rather different. The discrepancy between the experimental and the calculated weight loss is in part explained by the presence of remarkable amounts of C, H, and N in the residue (C: 12.29%, H: 0.27%, N: 3.19%; CHN_{sum}: 15.75%). Another reason for the differences

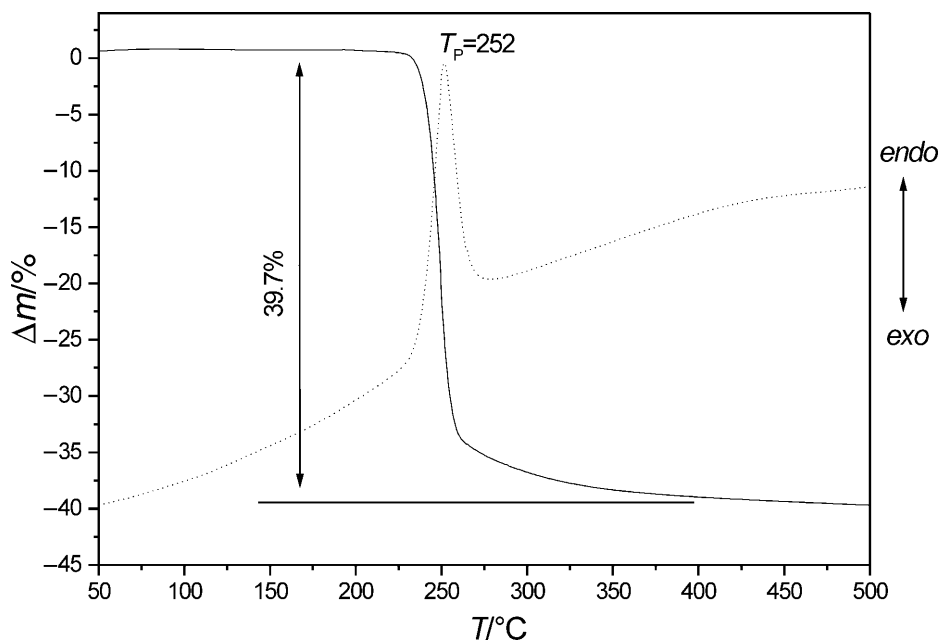


Fig. 5. DTA (dotted line) and TG (solid line) curves of $\text{Mn}(\text{dien})_2[\text{MoS}_4]$ (1)

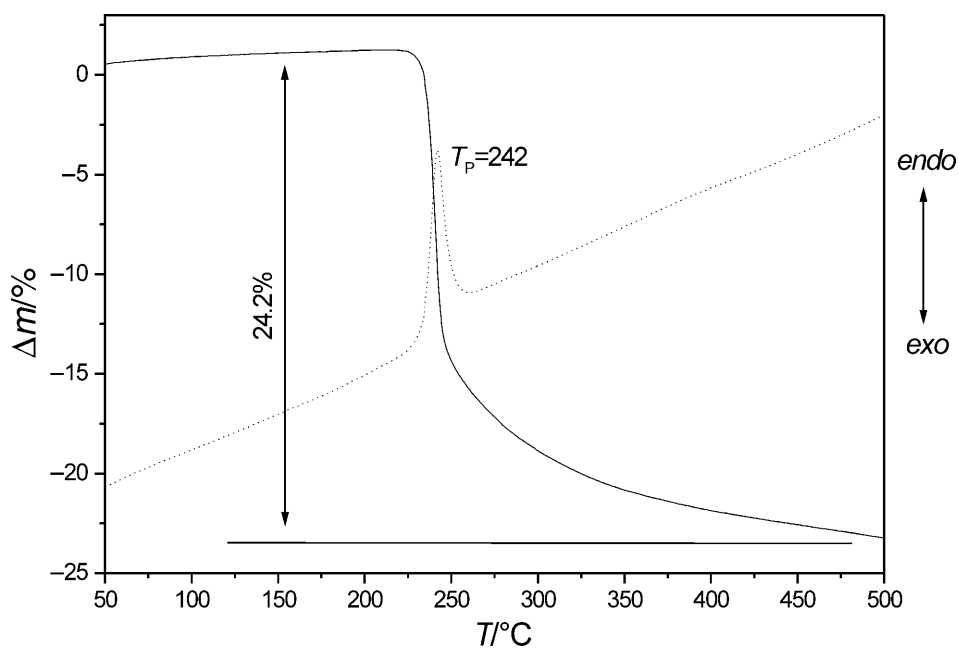


Fig. 6. DTA (dotted line) and TG (solid line) curves of $\text{Mn}(\text{dien})_2[\text{Mo}_2\text{O}_2\text{S}_6]$ (2)

between the observed and the calculated weight loss is that the exact composition of the binary molybdenum sulfide is not clear, and a sulfur-rich MoS_{2+x} may be formed during the thermal decomposition. In the decomposition products of both

compounds no organic amines could be detected by vibrational spectroscopy. Therefore, the reactions occurring during the decomposition are of a complex nature, involving redox reactions between the different atoms/molecules of the compounds.

It is worth to be mentioned that in the DTA curves no solid state isomerization of the [Mn(dien)₂]²⁺ complexes is observed before the decomposition, as it has been reported for other bis-dien transition metal complexes [39, 40].

Optical spectroscopy

The IR and Raman spectra of **1** and **2** in the region from 1700 to 140 cm⁻¹ are shown in Figs. 7 and 8. The spectra of the [MoS₄]²⁻ and [Mo₂O₂S₆]²⁻ anions are well understood [41, 42]. Differences in the anionic parts of the compounds can be easily seen from additional vibrations in the spectra of the oxothiomolybdate compared with the tetrathiomolybdate. In the Raman spectra of **1**, the ν(Mo–S) vibrations are observed at 466 and 453 cm⁻¹ and the δ(MoS₄) vibrations at 184 and 172 cm⁻¹. The Mo=O stretching mode in **2** is located in the region around 930 cm⁻¹, and the frequency of the terminal η²-disulfido group is found at 513 cm⁻¹ (IR) and 518 cm⁻¹ (Raman), respectively. The Mo–S vibrations in **2** are distinguishable in the Mo–S_{br} (S_{br}: bridging S atoms) modes (IR: from 464 to 359 cm⁻¹; Raman: 425 and 362 cm⁻¹) and in the Mo–S_t (S_t: terminal S atoms) which were observed at lower wave numbers (Raman: 281 and 259 cm⁻¹).

The vibrations of the [Mn(dien)₂]²⁺ cations are rather weak compared to the vibrations of the anions. However, the δ(NH₂) (**1**: 1576 cm⁻¹; **2**: 1585 cm⁻¹) and the δ(CH₂) (**1**: ~1460 cm⁻¹; **2**: ~1450 cm⁻¹) modes are perceptible in the infrared spectra [43].

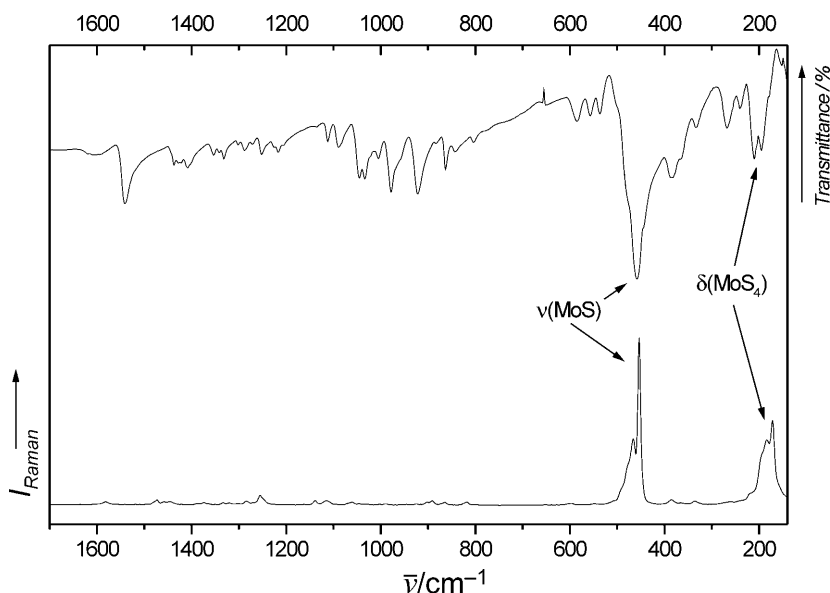


Fig. 7. Raman and IR spectra of Mn(dien)₂[MoS₄] (**1**)

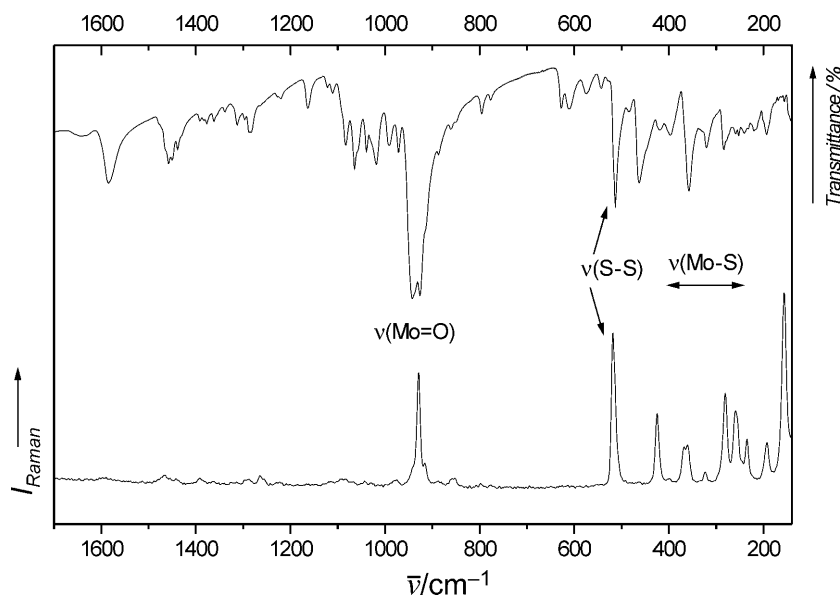


Fig. 8. Raman and IR spectra of $\text{Mn}(\text{dien})_2[\text{Mo}_2\text{O}_2\text{S}_6]$ (**2**)

Experimental

Syntheses

The compounds $\text{Mn}(\text{dien})_2[\text{MoS}_4]$ (**1**) and $\text{Mn}(\text{dien})_2[\text{Mo}_2\text{O}_2\text{S}_6]$ (**2**) were synthesized under similar conditions. Both syntheses were performed in teflon-lined steel autoclaves with an inner volume of 30 cm^3 . Compound **1** was obtained by the reaction of 0.5 mmol MnMoO_4 and 3 mmol S in 5 cm^3 diethylenetriamine (*dien*). The autoclave was heated at 120°C for six days and then cooled to room temperature within three hours. After washing with H_2O , red crystals of **1** were obtained as phase-pure product in nearly 95% yield (based on Mo). Compound **2** was also prepared by the reaction of 0.5 mmol MnMoO_4 and 3 mmol S , but in contrast to **1**, 5 cm^3 of an 20% aqueous diethylenetriamine solution were used as solvent. The mixture was also heated for six days at 120°C . The resulting compound $\text{Mn}(\text{dien})_2[\text{Mo}_2\text{O}_2\text{S}_6]$ was obtained phase-pure as orange platelet-like crystals with a yield of 50% (based on Mo). Both compounds are stable on air over a long time.

Crystal structure determination

Intensity data for both compounds were collected using a Philips PW1100 four-circle diffractometer operating in the ω - θ mode with graphite monochromated MoK_α radiation ($\lambda = 0.71073\text{ \AA}$). The measurements were carried out at 293 K. The raw intensities were corrected for Lorentz and polarization effects, and numerical absorption corrections using Ψ -scans were applied. The structures were solved with direct methods using the program SHELXS-97 [44], and refinement was done against F^2 using SHELXL-97 [45]. All heavy atoms were refined anisotropically. The carbon atoms in **1** are disordered with positions C1 (site occupation factor (*sof*) = 0.50), C1' (*sof* = 0.50), C2 (*sof* = 0.50), and C2' (*sof* = 0.50). The atom C1 in **2** is also slightly disordered with positions C1' (*sof* = 0.35) and C1 (*sof* = 0.65). The hydrogen atoms were positioned with idealized geometry and refined with fixed isotropic displacement parameters using a riding model. Due to the high symmetry of the space group the hydrogen atom H1 (bound to N1) in compound **1** is distributed over two positions with a site

Table 4. Technical details of data acquisition and selected refinement results for Mn(dien)₂[MoS₄] (1) and Mn(dien)₂[Mo₂O₂S₆] (2)

Compound	Mn(dien) ₂ MoS ₄	Mn(dien) ₂ [Mo ₂ O ₂ S ₆]
Space group	$\bar{1}4$	P2 ₁ /c
<i>a</i> /Å	10.219(2)	8.703(2)
<i>b</i> /Å	10.219(2)	18.390(4)
<i>c</i> /Å	9.259(2)	14.603(3)
β /°	90	103.18(3)
<i>V</i> /Å ³	966.9	2275.6
<i>Z</i>	2	4
<i>T</i> /K	293	293
μ /mm ⁻¹	1.73	2.20
<i>MW</i> /g · mol ⁻¹	485.5	677.5
Density (calc.)/g · cm ⁻³	1.667	1.978
2 θ range	5–60	5–56
Data collected	2251	7092
Unique data	1404	5487
Data (<i>F</i> _o > 4.0 σ (<i>F</i> _o))	1312	4285
<i>R</i> _{int}	0.0152	0.0164
$\Delta\rho$ /e · Å ⁻³	–0.36/0.37	–0.54/0.52
<i>R</i> ₁ (<i>F</i> _o > 4.0 σ (<i>F</i> _o)) ^a	0.0234	0.0231
<i>x</i>	0.0226	0.0251
<i>y</i>	0.53	0.59
<i>wR</i> ₂ ^b (all data) ^c	0.0545	0.0566
Goodness of fit	1.050	1.005
<i>Flack x</i> parameter	0.003(41)	–

^a $R_1 = \sum ||F_o| - |F_c|| / \sum |F_o|$; ^b $w = 1 / (\sigma^2(F_o^2) + (x \cdot P)^2 + y \cdot P)$, $P = (\max(F_o^2, 0) + 2 \cdot F_c^2) / 3$;
^c $wR_2 = (\sum (w(F_o^2 - F_c^2)^2) / \sum (w(F_o^2)^2))^{1/2}$

occupation factor of 0.5. Technical details of data acquisition and some selected refinement results are summarized in Table 4, selected bond lengths and angles in Tables 1 and 2.

Crystallographic data (excluding structure factors) for the structures reported in this paper have been deposited with the Cambridge Crystallographic Data Centre as supplementary publication no. CCDC 172836 for Mn(dien)₂[MoS₄] and CCDC 172835 for Mn(dien)₂[Mo₂O₂S₆]. Copies of the data can be obtained free of charge upon application to CCDC, 12 Union Road, Cambridge CB2 1EZ, UK. (fax: +44-(0)1223-336033, e-mail: deposit@ccdc.cam.ac.uk).

Physical methods

Thermal investigations were performed on a Netzsch 429 DTA-TG measurement device. The samples (initial weight about 50 mg) were heated in Al₂O₃ crucibles with a rate of 3°C/min up to 500°C and purged in an Ar stream of approximately 75 cm³/min.

Far-IR spectra (80 to 500 cm⁻¹) were measured on a Bruker IFS 66 infrared spectrometer in pressed polyethylene disks. MIR spectra of the compound were recorded in a KBr matrix. The sample was ground with dry KBr into a fine powder and pressed into a transparent pellet. The spectra were recorded in the region of 450 to 3000 cm⁻¹, resolution 1 cm⁻¹, with a ATI Mattson Genesis infrared spectrometer. Raman spectra were measured in the region from 100 to 3500 cm⁻¹ with a Bruker IFS 66 Fourier transform Raman spectrometer.

Acknowledgements

Financial support by the Federal State of Schleswig-Holstein and the *Deutsche Forschungsgemeinschaft* (DFG) is gratefully acknowledged.

References

- [1] Sheldrick WS, Wachhold MS (1997) *Angew Chem* **109**: 214; (1997) *Angew Chem Int Ed Engl* **36**: 206
- [2] Bowes CL, Ozin GA (1996) *Adv Mater* **8**: 13
- [3] Rabenau A (1985) *Angew Chem* **97**: 1017; (1985) *Angew Chem Int Ed Engl* **24**: 1026
- [4] Hille R (1996) *Chem Rev* **96**: 2757
- [5] Topsøe H, Massoth FE, Claussen BS (1996) Hydrotreating catalysis. In: Anderson JR, Boudart M (eds) *Catalysis-Science and Technology*, vol 11. Springer, Berlin
- [6] Bergmann H, Czeska B, Haas I, Katscher H, Mohsin B, Wandner KH (1995) *Mo Suppl.* In: *Gmelin Handbook of Inorganic and Organometallic Chemistry*, vol B8. Springer, Berlin
- [7] Picard S, Potel M, Gougeon P (1999) *Angew Chem* **111**: 2148; (1999) *Angew Chem Int Ed Engl* **38**: 2034
- [8] Müller A, Wittenbein V, Krickemeyer E, Bögge H, Lemke M (1991) *Z Anorg Allg Chem* **605**: 175
- [9] Coucouvanis D, Toupadakis A, Lane JD, Koo SM, Kim CG, Hadjikyriakou A (1991) *J Am Chem Soc* **113**: 5271
- [10] Hadjikyriakou AI, Coucouvanis D (1989) *Inorg Chem* **28**: 2169
- [11] Coucouvanis D, Hadjikyriakou A (1987) *Inorg Chem* **26**: 1
- [12] Ellermeier J, Näther C, Bensch W (1999) *Inorg Chem* **38**: 4601
- [13] von Zelewsky A (1996) *Stereochemistry of Coordination Compounds*. Wiley, Chichester
- [14] Okiyama K, Sato S, Saito Y (1979) *Acta Crystallogr* **B35**: 2389
- [15] Bruce DA, Wilkinson AP, White MG, Bertrand JA (1996) *J Solid State Chem* **125**: 228
- [16] Searle GH, Lincoln SF, Keene FR, Teague SG, Rowe DG (1977) *Aust J Chem* **30**: 1221
- [17] Searle GH, House DA (1987) *Aust J Chem* **40**: 361
- [18] House DA, McKee V, Robinson WT (1989) *Inorg Chim Acta* **157**: 15
- [19] Harada K (1993) *Bull Chem Soc Jpn* **66**: 2889
- [20] Stähler R, Näther C, Bensch W (2001) *Eur J Inorg Chem* 1835
- [21] Mukherjee AK, Koner S, Ghosh A, Chaudhuri NR, Mukherjee M, Welch AJ (1994) *J Chem Soc Dalton Trans* 2367
- [22] Rodríguez V, Gutiérrez-Zorrilla JM, Vitoria P, Luque A, Román P, Martínez-Ripoll M (1999) *Inorg Chim Acta* **290**: 57
- [23] Stähler R, Näther C, Bensch W (2001) *Acta Crystallogr* **C57**: 26
- [24] Bensch W, Näther C, Stähler R (2001) *Chem Commun* 477
- [25] Ellermeier J, Bensch W (2001) *Monatsh Chem* **132**: 565
- [26] Stephens FS (1969) *J Chem Soc A* 883 and 2233
- [27] Hodgson PG, Penfold BR (1974) *J Chem Soc Dalton Trans* 1870
- [28] Wendland F, Näther C, Bensch W (2000) *Z Naturforsch* **55b**: 871
- [29] Wendland F, Näther C, Bensch W (2000) *Z Anorg Allg Chem* **626**: 456
- [30] Schaefer H, Schaefer G, Weiss A (1964) *Z Naturforsch* **19b**: 76
- [31] Raymond CC, Dorhout PK, Miller SM (1995) *Z Kristallogr* **210**: 775
- [32] Ellermeier J, Näther C, Bensch W (1999) *Acta Crystallogr* **C55**: 501
- [33] Ellermeier J, Bensch W (2001) *Z Naturforsch* **56b**: 611
- [34] Clegg W, Sheldrick GM, Garner CD, Christou G (1980) *Acta Crystallogr* **B36**: 2784
- [35] Clegg W, Mohan N, Müller A, Neumann A, Rittner W, Sheldrick GM (1980) *Inorg Chem* **19**: 2066

- [36] Hu NH, Liu YS, Yan YZ, Xu JQ, Wei Q (1992) *J Struct Chem* **11**: 362
- [37] Alonso G, Del Valle M, Cruz J, Petranoskii V, Licea-Claverie A, Fuentes S (1998) *Catal Today* **43**: 117
- [38] Prasad TP, Diemann E, Müller A (1973) *J Inorg Nucl Chem* **35**: 1895
- [39] Koner S, Ghosh A, Chaudhuri NR (1988) *Transition Met Chem* **13**: 291
- [40] Koner S, Ghosh A, Chaudhuri NR (1990) *Transition Met Chem* **15**: 394
- [41] Müller A, Weinstock N, Schulze H (1972) *Spectochim Acta* **A28**: 1075
- [42] Fedin VP, Kolesov BA, Mironov YV, Gerasko OA, Fedorov VY (1991) *Polyhedron* **10**: 997
- [43] Schmidtke HH, Garthoff D (1968) *Inorg Chim Acta* **2**: 357
- [44] Sheldrick GM (1997) SHELXS97. Program for Crystal Structure Determination, Univ Göttingen, Germany
- [45] Sheldrick GM (1997) SHELXL97. Program for the Refinement of Crystal Structures, Univ Göttingen, Germany

Received November 5, 2001. Accepted December 27, 2001